Research Square

Preprints are preliminary reports that have not undergone peer review.
They should not be considered conclusive, used to inform clinical practice,
or referenced by the media as validated information.

CXCL13 Expressed on Inflamed Cerebral Blood Vessels Recruit IL-21 Producing T_{FH} Cells to Damage Neurons Following Stroke.

Aditya Rayasam
Medical College of Wisconsin https://orcid.org/0000-0003-1540-2654
Julie A. Kijak
University of Wisconsin-Madison
Lee Kissel
University of Wisconsin-Madison
Taehee Kim
University of Wisconsin-Madison
Martin Hsu
University of Wisconsin-Madison
Dinesh Joshi
University of Wisconsin-Madison
Collin J. Laaker
University of Wisconsin-Madison
Peter Cismaru
University of Wisconsin-Madison
Anders Lindstedt
University of Wisconsin-Madison
Krisztian Kovacs
University of Wisconsin-Madison
Raghu Vemuganti
University of Wisconsin-Madison
Shing Yan Chiu
University of Wisconsin-Madison
Thanthrige Thiunuwan Priyathilaka
University of Wisconsin-Madison
Matyas Sandor
University of Wisconsin-Madison
Zsuzsanna Fabry (zfabry@wisc.edu)
University of Wisconsin-Madison

Research

Keywords: lymphocytes, neuroinflammation, stroke, immune, brain, IL-21, T cells, neurons, apoptosis, MCAO

Posted Date: November 10th, 2021

DOI: https://doi.org/10.21203/rs.3.rs-1032310/v1

License: This work is licensed under a Creative Commons Attribution 4.0 International License.
Read Full License

Abstract

Background: Ischemic stroke is a leading cause of mortality worldwide, largely due to the inflammatory response to brain ischemia during post-stroke reperfusion. Despite ongoing intensive research, there have not been any clinically approved drugs targeting the inflammatory component to stroke. Preclinical studies have identified T cells as pro-inflammatory mediators of ischemic brain damage, yet mechanisms that regulate the infiltration and phenotype of these cells are lacking. Further understanding of how T cells migrate to the ischemic brain and facilitate neuronal death during brain ischemia can reveal novel targets for post-stroke intervention.

Methods: To identify the population of T cells that produce IL-21 and contribute to stroke, we performed transient middle cerebral artery occlusion (tMCAO) in mice and performed flow cytometry on brain tissue. We also utilized immunohistochemistry in both mouse and human brain sections to identify cell types and inflammatory mediators related to stroke-induced IL-21 signaling. To mechanistically demonstrate our findings, we employed pharmacological inhibitor anti-CXCL13 and performed histological analyses with Cresyl violet to evaluate its effects on brain infarct damage. Finally, to evaluate cellular mechanisms of stroke, we exposed mouse primary neurons to oxygen glucose deprivation (OGD) conditions with or without IL-21 and measured cell viability, caspase activity and JAK/STAT signaling.

Results: Flow cytometry on brains from mice following tMCAO identified a novel population of cells IL-21 producing CXCR5+ CD4+ ICOS-1+ T follicular helper cells (T_{FH}) in the ischemic brain early after injury. We observed augmented expression of CXCL13 on inflamed brain vascular cells and demonstrated that inhibition of CXCL13 protects mice from tMCAO by restricting the migration and influence of IL-21 producing T_{FH} cells in the ischemic brain. We also illustrate that neurons express IL-21R in the peri-infarct regions of both mice and human stroke tissue *in vivo.* Lastly, we found that IL-21 acts on mouse primary ischemic neurons to activate the JAK/STAT pathway and induce Caspase 3/7 mediated apoptosis *in vitro*.

Conclusion: These findings identify a novel mechanism for how pro-inflammatory T cells are recruited to the ischemic brain to propagate stroke damage and provide a potential novel therapeutic target for stroke.

Introduction

Stroke is one of the leading causes of death and disability worldwide. Despite ongoing intensive research, there has been limited translational success of pharmacological interventions and the only FDA approved therapy remains to be tissue plasminogen activator (tPA)[1]. One of the challenges of developing stroke therapies is the myriad of physiological mechanisms that occur within the patient following the disease, which include excitotoxicity, edema and inflammation among others [2-5]. Another challenge is the heterogeneous pathology from patient to patient due to the influence of age, sex, and other epidemiological heterogeneities [6-9].

While stroke incidence could be due to the hemorrhage of cerebral blood vessels, 87% of strokes are due to artery occlusions, which induce brain ischemia [6]. During ischemic stroke, occlusion of cerebral blood vessels deprives the brain of its required oxygen and nutrients to elicit the primary brain damage. Furthermore, once the occlusion is bypassed, peripheral blood containing pro-inflammatory immune cells reperfuse the once-occluded vessels to create secondary damage, which can oftentimes be more harmful than the occlusion-mediated damage itself. Several laboratories have attempted to identify the major pro-inflammatory cells and molecules responsible for most of the secondary tissue injury that occurs during the reperfusion phase of ischemic stroke [10-13].

T cells, in particular, have been identified to have a major role in ischemic stroke pathology and depending on the timing of the disease and their phenotype, T-cells can either be beneficial or harmful. Regulatory T cells have been demonstrated to be beneficial following stroke due their production of IL-10 [13-17]. Neuroprotective effects of IL-33 have been associated with its role in promoting the differentiation of anti-inflammatory TH_2 cells [18], although mice treated with IL-33 had exacerbated lung infection that led to greater functional deficits and mortality. Due to the application of different animal models and T-cell depletion strategies, controversies emerged regarding the function of some T-cell subtypes in ischemic brain injuries [14-20]. In spite of this, there is a consensus that T cells are detrimental in acute brain traumas. This is supported by data that mice deficient in lymphocytes are protected from acute tissue damage in ischemic injury [13, 20, 21]. We and others have identified that T cells can be recruited to the ischemic brain during the acute phase of stroke to augment brain damage. For example, IL-17 production by nonconventional γδ T cells has been implicated as well and its influence has been potentially attributed to its role in promoting neutrophil accumulation [11, 19, 20]. Furthermore, perforin, which is a pore forming cytolytic protein produced by cytotoxic T lymphocytes (CTLs) and NK cells, has also been implicated in influencing stroke outcome [21].

During the acute phase of ischemic stroke, CD4 produced IL-21 is a contributor to damage following transient middle cerebral artery occlusion (tMCAO) in mice and postmortem brain tissues from stroke patients contain IL21+ cells in perivascular regions of the ischemic brain parenchyma [22]. Given that work, we are now interested in the mechanism for how these IL-21 producing T cells infiltrate the ischemic brain during the reperfusion phase and amplify damage to the injured tissue. Several labs have identified some of the chemokine receptors involved in the recruitment of peripheral immune cells during the acute phase of stroke, which include CCR2, CCR7, CCR8, and CCR1 [23-29]. CXCR5, in particular, has been identified to play a role in mediating neuroinflammation and is upregulated in the ischemic brain following tMCAO in mice [30-33].

Identifying the targets of pro-inflammatory immune cells during the reperfusion phase of stroke can also lead to novel stroke therapies. Microglia, astrocytes, and endothelial cells have all been suggested to be targets of peripheral cytokines during neurological trauma [20, 34-42]. Limited work has identified neurons as direct targets of peripheral immune cell-produced cytokines but several studies have identified that local and peripheral myeloid cells, as well as astrocytes, can produce factors such as MMPs, IL-1β, TNFα, C1q, and C3a which can directly damage neurons following trauma [43-45]. Here, we show that

CXCL13 is upregulated on inflamed vascular cells, and that during reperfusion, IL-21 producing CD4+ ICOS-1+ CXCR5+ T_{FH} cells are recruited to the brain to deteriorate neurons and potentiate secondary stroke damage.

Materials And Methods

Ethics statement and Mice.

C57BL/6 WT mice and B6.IL-21-VFP knock in reporter mice (B6.Cg-*Il21*$^{tm1.1Hm}$/DcrJ) were obtained from Jackson Laboratory. All mice underwent SHAM or 1-hour occlusion and 4 hour or 24-hour reperfusion. All animal procedures used in this study were conducted in strict compliance with the National Institutes of Health Guide for the Care and Use of Laboratory Animals and approved by the University of Wisconsin Center for Health Sciences Research Animal Care Committee. All mice (~25 g) were anesthetized with 5% halothane for induction and 1.0% halothane for maintenance vaporized in N_2O and O_2 (3:2), and all efforts were made to minimize suffering. Male and Female mice between 10 weeks and 14 weeks were used for all studies.

Regional cerebral blood flow (rCBF) measurement.

Changes in rCBF at the surface of the left cortex were recorded using a blood perfusion monitor (Laserflo BPM2; Vasamedics) with a fiber optic probe (0.7 mm diam). The tip of the probe was fixed with glue on the skull over the core area supplied by the MCA (2 mm posterior and 6 mm lateral from bregma). Changes in rCBF after MCAO were recorded as a percentage of the baseline value. Mice included in these investigations had >80% relative decrease in rCBF during MCAO.

Investigation of intracranial vasculature.

Mice were anesthetized with ketamine (100 mg/kg, i.p.) and xylazine (10 mg/kg, i.p.). After thoracotomy was performed, a cannula was introduced into the ascending aorta through the left ventricle. Transcardial perfusion fixation was performed with 2 ml saline and 2 ml of 3.7% formaldehyde. Carbon lampblack (C198-500; Thermo Fisher Scientific) in an equal volume of 20% gelatin in ddH_2O (1 ml) was injected through the cannula. The brains were removed and fixed in 4% PFA overnight at 4°C. Posterior communicating arteries (PComA) connect vertebrobasilar arterial system to the Circle of Willis and internal carotid arteries, and its development affects brain sensitivity to ischemia among different mouse strains [46]. Development of PComA in both hemispheres was examined and graded on a scale of 0–3, as reported previously[47]: 0, no connection between anterior and posterior circulation; 1, anastomosis in capillary phase (present but poorly developed); 2, small truncal PComA; 3, truncal PComA.

Focal ischemia model.

Focal cerebral ischemia in mice was induced by occlusion of the left MCA, as described previously [48]. Operators performing surgeries were masked to experimental groups. In brief, the left common carotid

artery was exposed, and the occipital artery branches of the external carotid artery (ECA) were isolated and coagulated. After coagulation of the superior thyroid artery, the ECA was dissected distally and coagulated along with the terminal lingual and maxillary artery branches. The internal carotid artery (ICA) was isolated, and the extracranial branch of the ICA was then dissected and ligated. A standardized polyamide resin glue-coated 6.0 nylon monofilament (3021910; Doccol Corp) was introduced into the ECA lumen, and then advanced ~9–9.5 mm in the ICA lumen to block MCA blood flow. During the entire procedure, mouse body temperature was kept between 37 and 38°C with a heating pad. The suture was withdrawn 60 min after occlusion. The incision was closed, and the mice underwent recovery.

Infarct Measurement and Motor-Function Determination

Postischemic motor function was evaluated by the Rotarod test (4 min on a cylinder rotating at 8 rpm) as described previously[49]. On day 7, animals were killed by transcardiac 4% phosphate-buffered paraformaldehyde (PFA) perfusion. Each brain was postfixed, cryoprotected, and sectioned (coronal; 30 µm thickness at an interval of 320 µm). Serial sections were stained with cresyl violet and scanned using the National Institutes of Health ImageJ software. Ischemic infarct volume was estimated by numeric integration of data from five serial coronal sections in respect to the sectional interval as described previously [50, 51]. Each infarct volume was corrected to account for edema and differential shrinkage during tissue processing using the Swanson formula [52].

Lymphocyte isolation, and cytofluorometry (FACS).

Mice were deeply anesthetized with isoflurane and then transcardially perfused with cold PBS. Single cell suspensions were made from cervical lymph nodes (CLNs) and spleens by grinding the tissues between the frosted ends of glass slides[53]. Red blood cells were lysed using ACK lysis buffer, and cells were washed with HBSS. Brain and spinal cord tissues were minced with razor blades and pushed through 70 µm nylon cell strainers. Cells were washed, resuspended in 70% Percoll and overlaid with 30% Percoll. The gradient was centrifuged at 2400 rpm for 30 min at 4°C without brake. The interface was removed and washed before plating. All collected organs were weighed, and live cells were counted using a hemocytometer. Data were acquired on a BD LSR II flow cytometer (BD Biosciences) and analyzed using FlowJo software (Tree Star, Inc., Ashland, OR).

Fluorescent microscopy.

For frozen sections, mice were first perfused with cold PBS, followed by perfusion with 4% PFA/PBS. Harvested tissues were left in 25% sucrose/PBS overnight at 4°C. 10-40 µm-thick tissue cryosections were cut and stored at −80°C until staining. Floating sections were incubated in PBS 2 times for 10 minutes at room temperature before applying primary conjugated antibodies in FACS buffer (PBS/ with 2% BSA/ and 0.1% Sodium Azide) with 0.1% Triton X-100 (1:1000) overnight at 37°C. Sections were then washed 2 times for 10 min each time with PBS and secondary antibodies were applied in PBS (1:500) for 2 hours if necessary. Lastly, sections were washed 3 times for 10 min each time with PBS and mounted with ProLong Gold antifade reagent containing DAPI (Invitrogen). All images were acquired with a camera

(Optronics Inc., Goleta, CA) mounted on a fluorescence microscope (Olympus BX41, Leeds Precision Instruments). The brightness/contrast of the acquired digital images was applied equally across the entire image and equally to control images and analyzed using Adobe Photoshop CS4 software (Adobe Systems Inc., San Jose, CA).

Antibodies The following fluorophore-conjugated antibodies were purchased from BD Biosciences (Franklin Lakes, NJ): anti-CD4 (RM4-5), anti-ICOS-1 (D10.G4.1), anti-CXCR5 (2G8). All isotype controls were purchased from BD Biosciences. Anti-Fcγ-R (2.4G2) was produced from a hybridoma. IBA-1(019-19741) was purchased from WAKO (Richmond, VA). Anti-MAP2 (MAB8304) and anti-CXCL13 (AF470) were purchased from R and D systems (Minneapolis, MN). Anti-GFAP (AB5541), Anti-NeuN (MAB377B) and Anti-IL-21 (06-1074) was purchased from EDM Millipore (Hayward, CA). Anti-IL-21R (PA5-19982) was purchased from Invitrogen (Carlsbad, CA). JAK/STAT Phospho Antibody Array was purchased from Full Moon BioSystems (Sunnyvale, CA).

Oxygen glucose deprivation.

Primary neuronal cultures derived from embryonic day 14–18 mouse cortices were grown to 80% confluency in neural basal media supplemented with B27 (2%) and penicillin/streptomycin (1%), as previously described [54]. Astrocytic and microglial contamination was excluded based on the absence of $GFAP^+$ and $CD11b^+$ cells when stained by immunocytochemistry. For OGD, media was replaced with neural basal media with or without glucose and placed in a hypoxic chamber or under Normoxic conditions for 90 min at 37°C.

Human tissue samples.

Unidentified human brain samples were received from the Department of Pathology tissue bank and were exempt by IRB. Pathologists Dr. Krisztian Kovacs and Dr. Shahriar Salamat evaluated all acute human stroke tissue samples.

Statistical analyses and quality standards.

All surgeries were performed in a blinded manner and measurements masked where possible. Infarct volume measurements from Cresyl Violet stained sections were averaged from multiple independent blinded observers. Based on power calculations, n = 3–8 sex- and age-matched mice were used for each experiment and group assignment was randomized. Among animals receiving tMCAO procedure, 83% of WT mice were included in analysis as 17% displayed no injury. Mice were excluded due to premature death or vessel variation. Results are given as means ± s.e.m. Multiple comparisons were made using one-way ANOVA. Where appropriate, two-tailed nonparametric Mann-Whitney U test analysis was used for comparing measures made between two groups. P-values <0.05 were considered significant. *P < 0.05, **P < 0.01, ***P < 0.001, ****P < 0.0001. n.s. = not significant.

Results

T follicular helper cells infiltrate the ischemic brain.

Given our previously publish data showing that IL-21 produced CD4 T cells are damaging during the reperfusion phase of stroke, we sought to characterize these cells further. The combination of CD4, ICOS-1, CXCR5, and IL-21 is a signature of T follicular helper cells (T_{FH}) which have been identified to play an important role in helping B cells produce antibodies within B cell follicles of secondary lymph organs such as the lymph nodes, spleen and Peyer's patches [55, 56]. Nonetheless, while T_{FH} cells have been implicated to be involved in the pathology of CNS autoimmune diseases [56-59], to our knowledge, T_{FH} cells have never been identified in the ischemic brain. To determine whether these CD4+CXCR5+ cells were $T_{FH,}$ we sought to identify these cells comprehensively via flow cytometry [58, 60].

We first performed flow cytometry on isolated brain cells from SHAM operated mice and mice 4hrs, 24hrs and 4 days after tMCAO and identified a population of CD4+ICOS-1+ cells. On those double positive cells, we then gated on CXCR5 and for intracellular expression of IL-21 **(Fig. 1a).** Identification and quantification of the number of cells per gram tissue in brains harvested from SHAM and tMCAO mice revealed that CD4+ CXCR5+ ICOS-1+ IL-21+ cells are rapidly recruited to the ischemic brain within 4 hours after injury and are maintained in the ischemic brain up to 4 days **(Fig. 1b).** The percentage of CD4+ICOS-1+ cells that also expressed CXCR5+ and IL-21+ cells were also maintained up to 4 days after injury yet seemed to peak early after tMCAO. **(Fig. 1d).** These data identify CD4+ CXCR5+ ICOS-1+ IL-21+ cells after tMCAO and reveal their dynamics for entry intothe ischemic brain.

Cerebral blood vessels upregulate ICAM-1 and express CXCL13 in the ipsilateral brain hemisphere after tMCAO.

To understand the mechanism for how T_{FH} cellsare recruited the ischemic brain, we stained for CXCL13, the cognate ligand for CXCR5. Previously reports have identified that CXCL13 is expressed on ischemic blood vessels within the brain after stroke [33]. Here, we identified that cerebral vessels upregulate Intracellular Adhesion Molecule 1 (ICAM-1) and express CXCL13 4 hours and 24 hours after tMCAO. **(Fig. 2a).** Quantifications indicate that ICAM-1 expression is upregulated at 4 and 24 hours post tMCAO compared to SHAM in the peri-infarct area **(Fig. 2b).** Furthermore, co-localization of ICAM-1 and CXCL13 is also increased at both 4 hours and at 24 hours tMCAO compared to SHAM **(Fig. 2c)**. These data reveal that cerebral blood vessels up-regulate ICAM-1 and CXCL13 in the ipsilateral hemisphere as early as 4 hours after tMCAO ,revealing a potential mechanism for how CXCR5+ IL-21 producing T_{FH} cells are recruited to the ischemic brain.

We also assessed whether CXCR5+ CD4+ T cells were in the vicinity of CXCL13 expressing vessels following tMCAO. We observed abundant CD4 T cells in the peri-infarct region 4 hours after tMCAO with many of them also expressing CXCR5 (orange arrows) **(Fig 2d)**. These data demonstrate that CD4+ CXCR5+ cells are associated with CXCL13+ vessels in the ischemic brain.

Administration of anti-CXCL13 antibody reduces infarct volume following tMCAO.

Given that CXCR5 expressing T_{FH} cells migrate to the ischemic brain following tMCAO, we tested whether inhibiting CXCL13 could reduce T_{FH} cell recruitment and protect the brain after injury. To that end, we performed tMCAO on WT mice, administered anti-CXCL13 antibody (100 ug) i.p. or IgG2a isotype control within 5 minutes of reperfusion and evaluated the infarct volume at 24 hours tMCAO **(Fig. 3a).** Representative Cresyl Violet images and associated quantifications to depict the infarcted brain area revealed that anti-CXCL13 antibody treatment reduced the amount of ischemic brain damage at 24 hours tMCAO **(Fig. 3 b, c).**

We next performed flow cytometry on brains harvested from anti-CXCL13 treated and control treated 24-hour tMCAO mice to evaluate whether CXCL13 inhibition resulted in a decrease of IL-21 producing T_{FH} cell recruitment to brain. Representative gating and quantifications revealed the anti-CXCL13 antibody treatment did in fact reduce the amount of T_{FH} cells that infiltrated the ischemic brain at 24 hours tMCAO compared to IgG2a isotype control treatment **(Fig. 3d, e).** These data support that IL-21-producing T_{FH} cell infiltrate the CNS as a response to CXCL13 production by inflamed brain vessels.

CXCR5+ CD4+ T cells and CXCL13+ vessels localize to human acute stroke infarcts.

Given our data obtained in mice, we explored whether we could observe signatures of T_{FH} cell recruitment to the acute human ischemic brain tissue. We first performed hematoxylin and eosin (H&E) staining, which revealed the presence of immune cell clusters **(Fig. 4a)**. Further staining identified CXCR5+CD4+ T cells within those immune cell clusters, signature markers of T_{FH} cells **(Fig. 4b-e)**. Moreover, we also identified CXCL13+CD31+ vessels in the human ischemic brain tissue **(Fig. 4f-j)**. These data are congruent with our immunostaining in mice and suggest that mechanisms related to the contribution of T_{FH} cell to acute stroke pathology in mice may apply to humans as well.

IL-21R is upregulated in the ipsilateral brain hemisphere of mice 24 hours after tMCAO *in vivo* and in human stroke brains.

Given that we were able to clarify the mechanism for how IL-21 producing T_{FH} cells infiltrate the ischemic brain, our next question was to identify the cellular location of its cognate receptor, IL-21R within the brain. IL-21R has been widely described to be present on immune cells within the periphery but limited studies have identified its presence on cells within the CNS [61]. We stained 4-hour tMCAO brains to stain with NeuN and IL-21R in the ipsilateral brain hemisphere and contralateral hemisphere and observed that IL-21R is substantially more expressed in the ipsilateral hemisphere on neurons while there is minimal expression in the contralateral hemisphere **(Fig. 5a).** These data reveal that IL-21R gets upregulated in the infarcted brain hemisphere of mice *in vivo*. We then mapped out the co-localization of NeuN and IL-21R along coronal brain sections to get an understanding of the distribution of these double positive cells **(Fig. 5b)**. Quantification of the co-localization between NeuN and IL-21R along the coronal access revealed that the ipsilateral peri-infarct areas had significantly more NeuN cells that were also positive for IL-21R **(Fig. 5c)**. To test whether these NeuN+ IL-21R+ cells exist in ischemic brain tissue in our human samples, we stained human stroke tissue in the peri-infarct regions and in human control tissue.

Representative images and quantifications reveal that these NeuN+ IL-21R+ cells not only exist, but also have a higher prevalence in human stroke tissue versus control tissue **(Fig. 5d, e).** Overall, these data demonstrate that IL-21R is upregulated after tMCAO on ischemic neurons.

Administration of mIL-21 to primary neurons following OGD conditions induces Caspase 3/7 mediated apoptosis and activates JAK/STAT pathway.

To test whether IL-21 directly affects neurons, we isolated primary neurons from murine cortices. We then exposed primary neurons to 90 min of oxygen glucose deprivation (OGD) or normoxic conditions with mIL-21 for 24 hours in complete media to observe whether mIL-21 would affect neuronal morphology in hypoxic conditions. Representative images reveal that following OGD, exposure of neurons to complete media without mIL-21 had a baseline effect on the neuronal morphology but in a dose dependent manner, increasing concentrations of mIL-21 administration to OGD neurons correlated with decreased neuronal health **(Fig. 6a).** Quantification of the percentage of live neurons confirmed that exposure of 90 min OGD neurons to 24 hours of complete media with 10ng/ml mIL-21 significantly reduced the percentage of live cells compared to 24 hours of complete media alone. Additionally, increasing the exposure of 90 min OGD neurons to 24 hours of complete media with 100 ng/ml mIL-21 significantly reduced the percentage of live cells even further **(Fig. 6b).** These data indicate that IL-21R is upregulated on neurons and administration of mIL-21 dose dependently and directly potentiates neuronal death following OGD *in vitro.*

Next, we performed a flow cytometry assay to evaluate the levels of caspase 3/7 activity following IL-21 treatment. Representative histograms and quantifications revealed that IL-21 treatment following OGD conditions leads to increased Caspase 3/7 mediated apoptosis in the neurons **(Fig. 6c, d).** IL-21 has been shown to activate the JAK/STAT pathway in peripheral immune cells in several disease contexts including rheumatoid arthritis [62] and lymphoma [63]. Yet to our knowledge, the role of IL-21 signaling on hypoxic neurons has not been evaluated. To evaluate the downstream signaling of IL-21R activation on neurons, we performed a JAK/STAT phosphorylation signaling array. This array revealed that several JAK/STAT related proteins get phosphorylated at specific sites in response to OGD and IL-21 treatment compared to OGD conditions only, particularly JAK1 at Tyrosine1022 (Tyr1022), STAT3 at Serine727 (Ser727), and STAT5A at Tyrosine694 (Tyr694), which could be the mechanism for IL-21 induced caspase 3/7 mediated apoptosis in hypoxic neurons **(Fig. 6e, f)**.

Discussion

Here, we describe that following transient middle cerebral artery occlusion (tMCAO), CXCL13 is expressed by activated cerebral blood vessels, which contributes to the recruitment of CD4+ ICOS-1+ CXCR5+ IL-21 producing T follicular helper cells (T_{FH}) into the brain during the reperfusion phase of the disease. Once these T_{FH} cells enter the brain, they then augment ischemic brain damage by producing IL21 that directly targets IL-21R bearing neurons potentially by activating the JAK/STAT pathway. Disruption of this pathway, by blocking chemotaxis of T_{FH} to the ischemic brain via antibody-mediated blocking of CXCL13

protects mice from tMCAO mediated brain damage. Overall, these data identify a novel mechanism for how pro-inflammatory T_{FH} cells are recruited to the ischemic brain and elicit their damage during murine stroke and identify potential novel targets for stroke therapy.

The combination of CD4, ICOS-1, CXCR5, and IL-21 is a signature of T_{FH} which have been identified to play an important role in helping B cells produce antibodies within B cell follicles of secondary lymph organs such as the lymph nodes, spleen and Peyer's patches [55, 56]. Yet, while T_{FH} cells have been implicated to be involved in the pathology of CNS diseases [59, 64], to our knowledge, T_{FH} cells have never been identified in the ischemic brain. CXCL13 is considered to be a B lymphocyte recruiting chemokine and is primarily expressed in lymphoid organs so why it gets upregulated in the ischemic brain is unknown. Given the literature implicating interactions with Tfh cells, CXCL13 and B cells, we measured B cells in the tMCAO brain early after tMCAO but only identified a marginal subset of these cells 4 hours and 24 hours after injury compared to T cells [5]. Doyle et al. conducted a study to show that B cells contribute to delayed cognitive impairment following distal MCAO in mice [65]. Moreover, our data demonstrate that Tfh cells are maintained in the ischemic brain days after tMCAO. Therefore, we aim to assess whether interaction between Tfh cells and B cells could mediate B cell-mediated neurotoxic responses in subsequent studies.

CXCL13 has been observed to be expressed in the meninges of the CNS during autoimmune diseases and has emerged as a candidate as a therapeutic target for multiple sclerosis (MS)[30, 66-68]. In MS lesions, CXCL13 has been identified particularly in glial cells [69]; while during ischemic brain conditions, CXCL13 is mainly expressed on cerebral blood vessels [33]. Since glial cell death has been identified as a potential inducer of CNS autoimmunity [5, 70, 71], and blood brain barrier breakdown is one of the primary events that occur following ischemic brain damage [41, 72], CXCL13 may be a ubiquitous danger signal that gets upregulated to license peripheral immune cells for CNS entry. Our data indicates that CXCL13 is expressed in stroke patients brain adjacent to the ischemic injury regions, indicating the importance of this chemokine in disease pathogenesis in humans. Evaluating the therapeutic window for when disrupting the CXCL13-CXCR5 axis could reduce stroke damage *in vivo* is of future interest.

Since the signature cytokine of T_{FH} cells is IL-21, we searched for IL-21R expressing cells in the ischemic tissue and identified IL-21R expression on hypoxic neurons following tMCAO. IL-21R expression has been widely reported on a myriad of cell types in the periphery and can play various roles that alter functional outcome depending on the target cell. [61]. Interestingly, there has been limited knowledge of IL-21R expression in CNS cells [73]. Recently, the Marchuck group reported that global deletion of IL-21R in mice is detrimental to stroke outcome following permanent MCAO (pMCAO) [74]. Although our data seems contradictory this study, there are several factors that could contribute to the different findings. Mainly, the pathology in the permanent MCAO murine model is well-known to be less dependent on peripheral immune cells compared to the tMCAO model, so the role of T cell-derived IL-21 in their findings is likely more limited [5]. Moreover, their work concludes that local CNS cells produce IL-21 to produce a beneficial effect on hypoxic neurons whereas in our model, IL-21 is produced by infiltrating T cells, which

have a much higher capacity to produce this cytokine. Given the double-edged sword nature of IL-21, it is possible that low levels of IL-21 could be protective on hypoxic neurons and high levels could be detrimental. To test this hypothesis, we dose-dependently administered mIL-21 to neurons and show that at 10ng/ml, and 100ng/ml, increasing concentrations of mIL-21 result in increasing amounts of neuronal death. Interestingly, at 1ng/ml, we do see a protective effect on hypoxic neurons relative to untreated hypoxic neurons albeit not statistically significant**.** These studies highlight the importance of understanding how therapies designed based on specific murine models could translate to patients based on their specific clinical signs and biomarkers.

Elucidating how common gamma chain cytokine receptors like IL-21R initiate the activation of the JAK/STAT pathway can be key in understanding how cytokines influence pathology. Often the same cytokine can elicit divergent responses depending on the timing and downstream effects on JAK/STAT related phosphorylation [75]. In our study, IL-21 had the largest effect on the phosphorylating at STAT3(Ser727), STAT5A(Tyr694), and JAK(Tyr1022) which led to caspase-mediated apoptosis in hypoxic neurons. Whether all or some of these phosphorylation events are required for caspase-mediated apoptosis is unknown.

In conclusion, our work is the first to identify a mechanism for how IL-21 producing T cells enter the ischemic brain and how these cells damage the inflamed tissue during the reperfusion phase of stroke. Future studies entail developing pharmacological tools that target neuronal IL-21R specifically and exploring the role of Tfh in the ischemic brain at later time points. Moreover, revealing what regulates IL-21R expression on neurons following hypoxic conditions and understanding the influence on the JAK/STAT pathway can help us delineate the potential beneficial effects from the harmful ones to limit the potential issues with the double-edged nature of IL-21 signaling. While features of our murine data are evident in human acute ischemic stroke tissue, we hope that findings from this work will lead to novel therapies for stroke patients.

Abbreviations

tMCAO: transient middle cerebral artery occlusion

T_{FH}: T follicular helper cells

IL: Interleukin

OGD: Oxygen glucose deprivation

tPA: tissue plasminogen activator

FDA: Food and drug administration

rCBF: Regional cerebral blood flow

PComA: Posterior communicating arteries

ECA: External carotid artery

ICA: Internal carotid artery

MCA: Middle cerebral artery

CLN: Cervical lymph nodes

MAP2: Microtubule associated protein 2

Declarations

Ethics approval

C57BL/6 WT mice were obtained from The Jackson Laboratory (Bar Harbor, ME). All animal procedures used in this study were conducted in strict compliance with the National Institutes of Health Guide for the Care and Use of Laboratory Animals and approved by the University of Wisconsin Center for Health Sciences Research Animal Care Committee. All mice (~25 g) were anesthetized with isoflurane for procedures, and all efforts were made to minimize suffering.

Consent for publication

All others approved the manuscript and associated data.

Availability of data and materials

The data that support the findings of this study are available from the corresponding author upon request.

Competing Interests

No competing interests

Funding

This research was supported by NIH/NIGMS grant T32 GM007507 (Neuroscience Training Program), NIH grants R01-NS37570 (Z.Fabry) and R01-AI048087 (M. Sandor), and AHA pre-doctoral grant 1525500022 (A. Rayasam).

Author Contributions

A.R., J.A.K., and T.K. performed tMCAO surgeries. A.R., J.A.K, L.K. and A.L. analyzed immune responses and histological data. J.A.K., M.H., C.L., P.C, T.P. and A.L. helped perform immunohistochemistry and analyses and assisted with murine organ harvests. L.K. and K.K. performed IHC and analyses on human

tissue. D.J. generated primary neurons. R.V., S.L. Z.F., and M.S. provided critical conceptual guidance, comments and reviews. A.R. and Z.F. wrote the main manuscript text. A.R. prepared figures. All authors reviewed the manuscript.

Acknowledgements

We would like to thank Khen Macvilay, Laura Schmitt Brunold, and Satoshi Kinoshita for excellent technical assistance. We would also like to thank Eric Silignavong and Dr. Christian Gerhart for assistance.

References

1. Papadopoulos, S.M., et al., *Recombinant human tissue-type plasminogen activator therapy in acute thromboembolic stroke.* J Neurosurg, 1987. **67**(3): p. 394-8.
2. Belayev, L., et al., *Middle cerebral artery occlusion in the rat by intraluminal suture. Neurological and pathological evaluation of an improved model.* Stroke, 1996. **27**(9): p. 1616-22; discussion 1623.
3. Rodrigues, S.F. and D.N. Granger, *Blood cells and endothelial barrier function.* Tissue Barriers, 2015. **3**(1-2): p. e978720.
4. Weilinger, N.L., et al., *Ionotropic receptors and ion channels in ischemic neuronal death and dysfunction.* Acta Pharmacol Sin, 2013. **34**(1): p. 39-48.
5. Rayasam, A., et al., *Contrasting roles of immune cells in tissue injury and repair in stroke: The dark and bright side of immunity in the brain.* Neurochem Int, 2017.
6. Rothwell, P.M., et al., *Change in stroke incidence, mortality, case-fatality, severity, and risk factors in Oxfordshire, UK from 1981 to 2004 (Oxford Vascular Study).* Lancet, 2004. **363**(9425): p. 1925-33.
7. Engel, O., et al., *Modeling stroke in mice - middle cerebral artery occlusion with the filament model.* J Vis Exp, 2011(47).
8. Siebenhofer, A., et al., *Primary care management for optimized antithrombotic treatment [PICANT]: study protocol for a cluster-randomized controlled trial.* Implement Sci, 2012. **7**: p. 79.
9. Werner, M., et al., *Anatomic variables contributing to a higher periprocedural incidence of stroke and TIA in carotid artery stenting: single center experience of 833 consecutive cases.* Catheter Cardiovasc Interv, 2012. **80**(2): p. 321-8.
10. Felger, J.C., et al., *Brain dendritic cells in ischemic stroke: time course, activation state, and origin.* Brain Behav Immun, 2010. **24**(5): p. 724-37.
11. Gelderblom, M., P. Arunachalam, and T. Magnus, *gammadelta T cells as early sensors of tissue damage and mediators of secondary neurodegeneration.* Front Cell Neurosci, 2014. **8**: p. 368.
12. Hurn, P.D., et al., *T- and B-cell-deficient mice with experimental stroke have reduced lesion size and inflammation.* J Cereb Blood Flow Metab, 2007. **27**(11): p. 1798-805.
13. Kleinschnitz, C., et al., *Regulatory T cells are strong promoters of acute ischemic stroke in mice by inducing dysfunction of the cerebral microvasculature.* Blood, 2013. **121**(4): p. 679-91.

14. Liesz, A., et al., *Regulatory T cells are key cerebroprotective immunomodulators in acute experimental stroke.* Nat Med, 2009. **15**(2): p. 192-9.
15. Stubbe, T., et al., *Regulatory T cells accumulate and proliferate in the ischemic hemisphere for up to 30 days after MCAO.* J Cereb Blood Flow Metab, 2013. **33**(1): p. 37-47.
16. Brea, D., et al., *Regulatory T cells modulate inflammation and reduce infarct volume in experimental brain ischaemia.* J Cell Mol Med, 2014. **18**(8): p. 1571-9.
17. Na, S.Y., et al., *Amplification of regulatory T cells using a CD28 superagonist reduces brain damage after ischemic stroke in mice.* Stroke, 2015. **46**(1): p. 212-20.
18. Luo, Y., et al., *Interleukin-33 ameliorates ischemic brain injury in experimental stroke through promoting Th2 response and suppressing Th17 response.* Brain Res, 2015. **1597**: p. 86-94.
19. Shichita, T., et al., *Pivotal role of cerebral interleukin-17-producing gammadeltaT cells in the delayed phase of ischemic brain injury.* Nat Med, 2009. **15**(8): p. 946-50.
20. Derkow, K., et al., *Microglia Induce Neurotoxic IL-17+ gammadelta T Cells Dependent on TLR2, TLR4, and TLR9 Activation.* PLoS One, 2015. **10**(8): p. e0135898.
21. Mracsko, E., et al., *Antigen dependently activated cluster of differentiation 8-positive T cells cause perforin-mediated neurotoxicity in experimental stroke.* J Neurosci, 2014. **34**(50): p. 16784-95.
22. Clarkson, B.D., et al., *T cell-derived interleukin (IL)-21 promotes brain injury following stroke in mice.* J Exp Med, 2014. **211**(4): p. 595-604.
23. Dimitrijevic, O.B., et al., *Effects of the chemokine CCL2 on blood-brain barrier permeability during ischemia-reperfusion injury.* J Cereb Blood Flow Metab, 2006. **26**(6): p. 797-810.
24. Offner, H., et al., *Experimental stroke induces massive, rapid activation of the peripheral immune system.* J Cereb Blood Flow Metab, 2006. **26**(5): p. 654-65.
25. Yan, Y.P., et al., *Monocyte chemoattractant protein-1 plays a critical role in neuroblast migration after focal cerebral ischemia.* J Cereb Blood Flow Metab, 2007. **27**(6): p. 1213-24.
26. Brait, V.H., et al., *Chemokine-related gene expression in the brain following ischemic stroke: no role for CXCR2 in outcome.* Brain Res, 2011. **1372**: p. 169-79.
27. Gliem, M., et al., *Macrophages prevent hemorrhagic infarct transformation in murine stroke models.* Ann Neurol, 2012. **71**(6): p. 743-52.
28. Stowe, A.M., et al., *CCL2 upregulation triggers hypoxic preconditioning-induced protection from stroke.* J Neuroinflammation, 2012. **9**: p. 33.
29. Tokami, H., et al., *RANTES has a potential to play a neuroprotective role in an autocrine/paracrine manner after ischemic stroke.* Brain Res, 2013. **1517**: p. 122-32.
30. Huber, A.K. and D.N. Irani, *Targeting CXCL13 During Neuroinflammation.* Adv Neuroimmune Biol, 2015. **6**(1): p. 1-8.
31. Zhang, Q., et al., *Chemokine CXCL13 mediates orofacial neuropathic pain via CXCR5/ERK pathway in the trigeminal ganglion of mice.* J Neuroinflammation, 2016. **13**(1): p. 183.

32. Ortega, S.B., et al., *Stroke induces a rapid adaptive autoimmune response to novel neuronal antigens.* Discov Med, 2015. **19**(106): p. 381-92.
33. Monson, N.L., et al., *Repetitive hypoxic preconditioning induces an immunosuppressed B cell phenotype during endogenous protection from stroke.* J Neuroinflammation, 2014. **11**: p. 22.
34. Ritzel, R.M., et al., *Functional differences between microglia and monocytes after ischemic stroke.* J Neuroinflammation, 2015. **12**: p. 106.
35. Wang, S., H. Zhang, and Y. Xu, *Crosstalk between microglia and T cells contributes to brain damage and recovery after ischemic stroke.* Neurol Res, 2016. **38**(6): p. 495-503.
36. Wu, M.H., et al., *Inhibition of Peripheral TNF-alpha and Downregulation of Microglial Activation by Alpha-Lipoic Acid and Etanercept Protect Rat Brain Against Ischemic Stroke.* Mol Neurobiol, 2016. **53**(7): p. 4961-71.
37. Zacharek, A., et al., *Angiopoietin1/Tie2 and VEGF/Flk1 induced by MSC treatment amplifies angiogenesis and vascular stabilization after stroke.* J Cereb Blood Flow Metab, 2007. **27**(10): p. 1684-91.
38. Cekanaviciute, E., et al., *Astrocytic transforming growth factor-beta signaling reduces subacute neuroinflammation after stroke in mice.* Glia, 2014. **62**(8): p. 1227-40.
39. Wang, M., et al., *Damage effect of interleukin (IL)-23 on oxygen-glucose-deprived cells of the neurovascular unit via IL-23 receptor.* Neuroscience, 2015. **289**: p. 406-16.
40. Zhang, Z.G., et al., *VEGF enhances angiogenesis and promotes blood-brain barrier leakage in the ischemic brain.* J Clin Invest, 2000. **106**(7): p. 829-38.
41. Knowland, D., et al., *Stepwise recruitment of transcellular and paracellular pathways underlies blood-brain barrier breakdown in stroke.* Neuron, 2014. **82**(3): p. 603-17.
42. Vafadari, B., A. Salamian, and L. Kaczmarek, *MMP-9 in translation: from molecule to brain physiology, pathology, and therapy.* J Neurochem, 2016. **139 Suppl 2**: p. 91-114.
43. Arango-Davila, C.A., et al., *Soluble or soluble/membrane TNF-alpha inhibitors protect the brain from focal ischemic injury in rats.* Int J Neurosci, 2015. **125**(12): p. 936-40.
44. Gautier, S., et al., *Impact of the neutrophil response to granulocyte colony-stimulating factor on the risk of hemorrhage when used in combination with tissue plasminogen activator during the acute phase of experimental stroke.* J Neuroinflammation, 2014. **11**: p. 96.
45. Alawieh, A., A. Elvington, and S. Tomlinson, *Complement in the Homeostatic and Ischemic Brain.* Front Immunol, 2015. **6**: p. 417.
46. Barone, F.C., et al., *Mouse strain differences in susceptibility to cerebral ischemia are related to cerebral vascular anatomy.* J Cereb Blood Flow Metab, 1993. **13**(4): p. 683-92.
47. Majid, A., et al., *Differences in vulnerability to permanent focal cerebral ischemia among 3 common mouse strains.* Stroke, 2000. **31**(11): p. 2707-14.
48. Longa, E.Z., et al., *Reversible middle cerebral artery occlusion without craniectomy in rats.* Stroke, 1989. **20**(1): p. 84-91.

49. Nakka, V.P., et al., *Increased cerebral protein ISGylation after focal ischemia is neuroprotective.* J Cereb Blood Flow Metab, 2011. **31**(12): p. 2375-84.
50. Kim, T., et al., *Poststroke Induction of alpha-Synuclein Mediates Ischemic Brain Damage.* J Neurosci, 2016. **36**(26): p. 7055-65.
51. Mehta, S.L., T. Kim, and R. Vemuganti, *Long Noncoding RNA FosDT Promotes Ischemic Brain Injury by Interacting with REST-Associated Chromatin-Modifying Proteins.* J Neurosci, 2015. **35**(50): p. 16443-9.
52. Swanson, R.A., et al., *A semiautomated method for measuring brain infarct volume.* J Cereb Blood Flow Metab, 1990. **10**(2): p. 290-3.
53. Harris, M.G., et al., *Immune privilege of the CNS is not the consequence of limited antigen sampling.* Sci Rep, 2014. **4**: p. 4422.
54. Kintner, D.B., et al., *Excessive Na+/H+ exchange in disruption of dendritic Na+ and Ca2+ homeostasis and mitochondrial dysfunction following in vitro ischemia.* J Biol Chem, 2010. **285**(45): p. 35155-68.
55. Fazilleau, N., et al., *Follicular helper T cells: lineage and location.* Immunity, 2009. **30**(3): p. 324-35.
56. Nurieva, R.I., et al., *Bcl6 mediates the development of T follicular helper cells.* Science, 2009. **325**(5943): p. 1001-5.
57. Akiba, H., et al., *The role of ICOS in the CXCR5+ follicular B helper T cell maintenance in vivo.* J Immunol, 2005. **175**(4): p. 2340-8.
58. Baumjohann, D., T. Okada, and K.M. Ansel, *Cutting Edge: Distinct waves of BCL6 expression during T follicular helper cell development.* J Immunol, 2011. **187**(5): p. 2089-92.
59. Kielczewski, J.L., et al., *Tertiary Lymphoid Tissue Forms in Retinas of Mice with Spontaneous Autoimmune Uveitis and Has Consequences on Visual Function.* J Immunol, 2016. **196**(3): p. 1013-25.
60. Baumjohann, D. and K.M. Ansel, *Tracking early T follicular helper cell differentiation in vivo.* Methods Mol Biol, 2015. **1291**: p. 27-38.
61. Spolski, R. and W.J. Leonard, *Interleukin-21: a double-edged sword with therapeutic potential.* Nat Rev Drug Discov, 2014. **13**(5): p. 379-95.
62. Zhang, M., et al., *Selective targeting of JAK/STAT signaling is potentiated by Bcl-xL blockade in IL-2-dependent adult T-cell leukemia.* Proc Natl Acad Sci U S A, 2015. **112**(40): p. 12480-5.
63. Bhatt, S., K.A. Sarosiek, and I.S. Lossos, *Interleukin 21 - its potential role in the therapy of B-cell lymphomas.* Leuk Lymphoma, 2017. **58**(1): p. 17-29.
64. Phares, T.W., et al., *CXCL13 promotes isotype-switched B cell accumulation to the central nervous system during viral encephalomyelitis.* Brain Behav Immun, 2016. **54**: p. 128-39.
65. Doyle, K.P., et al., *B-lymphocyte-mediated delayed cognitive impairment following stroke.* J Neurosci, 2015. **35**(5): p. 2133-45.
66. Corcione, A., et al., *Recapitulation of B cell differentiation in the central nervous system of patients with multiple sclerosis.* Proc Natl Acad Sci U S A, 2004. **101**(30): p. 11064-9.

67. Kowarik, M.C., et al., *CXCL13 is the major determinant for B cell recruitment to the CSF during neuroinflammation.* J Neuroinflammation, 2012. **9**: p. 93.
68. Puthenparampil, M., et al., *BAFF Index and CXCL13 levels in the cerebrospinal fluid associate respectively with intrathecal IgG synthesis and cortical atrophy in multiple sclerosis at clinical onset.* J Neuroinflammation, 2017. **14**(1): p. 11.
69. Krumbholz, M., et al., *Chemokines in multiple sclerosis: CXCL12 and CXCL13 up-regulation is differentially linked to CNS immune cell recruitment.* Brain, 2006. **129**(Pt 1): p. 200-11.
70. Way, S.W. and B. Popko, *Harnessing the integrated stress response for the treatment of multiple sclerosis.* Lancet Neurol, 2016. **15**(4): p. 434-43.
71. Traka, M., et al., *Oligodendrocyte death results in immune-mediated CNS demyelination.* Nat Neurosci, 2016. **19**(1): p. 65-74.
72. Zhang, H.T., et al., *Early VEGF inhibition attenuates blood-brain barrier disruption in ischemic rat brains by regulating the expression of MMPs.* Mol Med Rep, 2017. **15**(1): p. 57-64.
73. Tzartos, J.S., et al., *IL-21 and IL-21 receptor expression in lymphocytes and neurons in multiple sclerosis brain.* Am J Pathol, 2011. **178**(2): p. 794-802.
74. Lee, H.K., et al., *Natural allelic variation of the IL-21 receptor modulates ischemic stroke infarct volume.* J Clin Invest, 2016. **126**(8): p. 2827-38.
75. Wan, C.K., et al., *Opposing roles of STAT1 and STAT3 in IL-21 function in CD4+ T cells.* Proc Natl Acad Sci U S A, 2015. **112**(30): p. 9394-9.

Figures

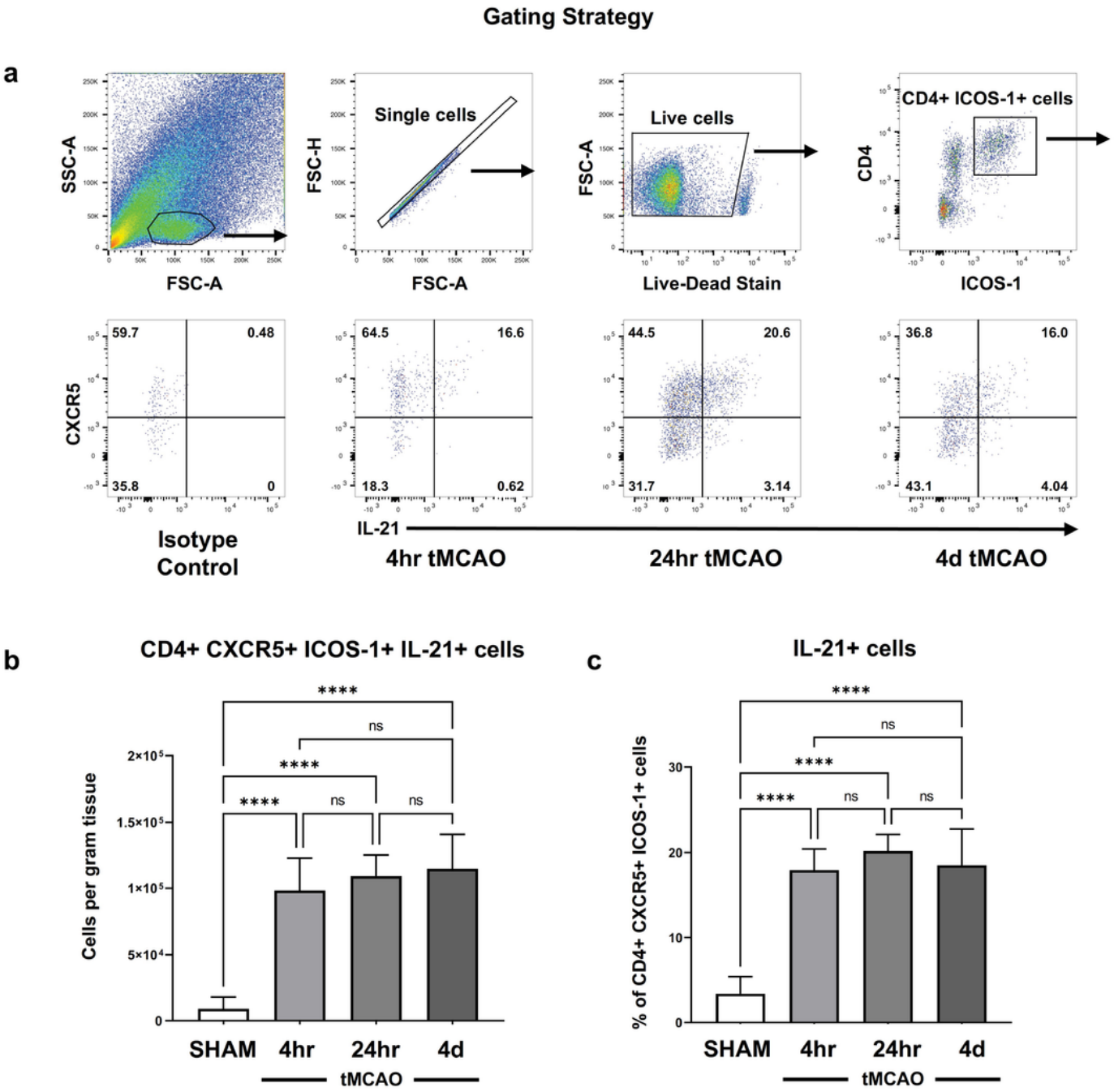

Figure 1

T follicular helper cells infiltrate the ischemic brain. (a) Representative gating from brains harvested from SHAM mice, 4 hour (hr) tMCAO, 24hr tMCAO, and 4 day(d) tMCAO mice. Following gating on single cells and live cells, we subsequently gated on cells double positive for CD4 and ICOS-1. From the double positive CD4+ ICOS-1+ cells, CXCR5 and IL-21 was gated based on isotype control for IL-21. (b) Quantification of CD4+ CXCR5+ ICOS-1+IL-21+ cells in brains of SHAM mice, 4hr, 24hr, and 4d tMCAO

mice (n=6). (c) Quantification of CXCR5+ IL-21+ cells in brains of SHAM mice, 4hr, 24hr and 4d after tMCAO mice (n=6). Data represent mean ± s.e.m. *P < 0.05, **P < 0.01, ***P < 0.001, ****P < 0.0001. n.s. = not significant. One-way ANOVA followed by Dunn's post-hoc test (b,c).

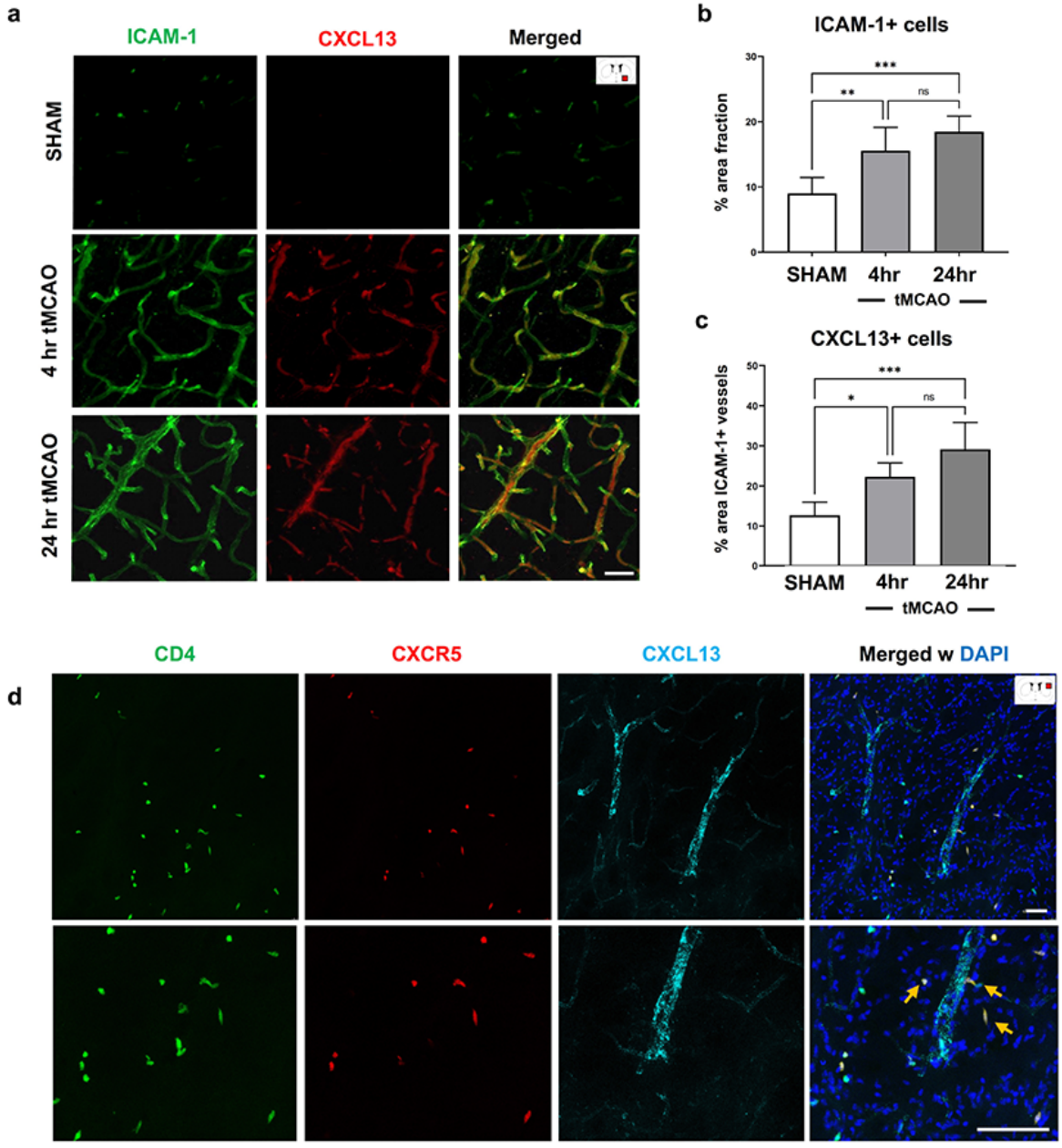

Figure 2

Cerebral blood vessel upregulation of ICAM-1 and CXCL13 in the ipsilateral brain hemisphere after tMCAO (a) Representative images stained with ICAM-1 (green), CXCL13 (red), and Merged (right panel) of

cerebral blood vessels in ipsilateral brain hemisphere 4hr and 24hr after tMCAO in mice. (b) Quantification of ICAM-1+ area in ipsilateral brain hemisphere following SHAM conditions, at 4hr tMCAO and at 24hr tMCAO in mice (n=5). (c) Quantification of percentage area of ICAM-1 vessels that are also CXCL13+ in ipsilateral brain hemisphere following SHAM conditions, at 4hr tMCAO and at 24hr tMCAO in mice. (d) Representative low and high magnification images of CD4 (green), CXCR5 (red), and CXCL13 (cyan) 4hrs after tMCAO in the peri-infarct area. Orange arrows depict some of the CD4+ CXCR5+ double positive cells. Scale bar = 30 μm. Data represent mean ± s.e.m. *P < 0.05, **P < 0.01, ***P < 0.001, ****P < 0.0001. n.s. = not significant. One-way ANOVA followed by Dunn’s post-hoc test (b, c).

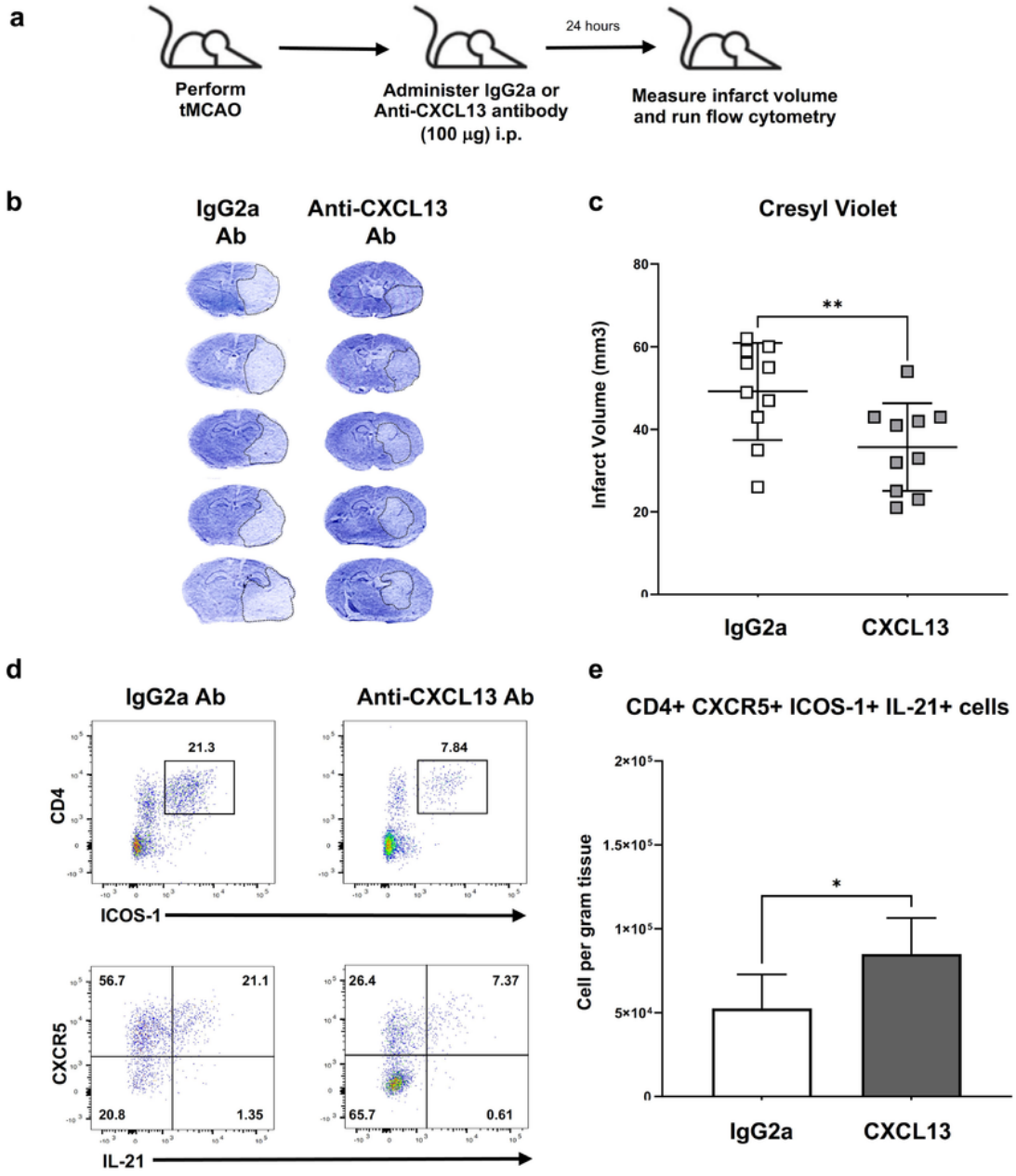

Figure 3

Administration of anti-CXCL13 antibody reduces infarct volume following tMCAO. (a) Experimental design for administration of IgG2a and anti-CXCL13 antibody (100 mg) i.p. (b) Representative Cresyl Violet images to assess ischemic brain damage at 24hr tMCAO in IgG2a treated and anti-CXCL13 antibody (100 mg) treated mice. (c) Quantification of infarct volume (mm3) at 24hr tMCAO in IgG2a treated and CXCL13 antibody treated mice (n=10). (d) Representative flow cytometry gating of

CD4+ICOS-1+ CXCR5+ IL-21+ cells from IgG2a isotype control treated and anti-CXCL13 antibody treated mice (top) at 24hr tMCAO. (e) Quantification of CD4+ CXCR5+ ICOS-1+ IL-21+ cells from IgG2a isotype control treated and anti-CXCL13 antibody treated mice at 24hr tMCAO. (n=6) Data represent mean ± s.e.m. *P < 0.05, **P < 0.01, ***P < 0.001, ****P < 0.0001. Student's t test with Mann-Whitney U test (c, e).

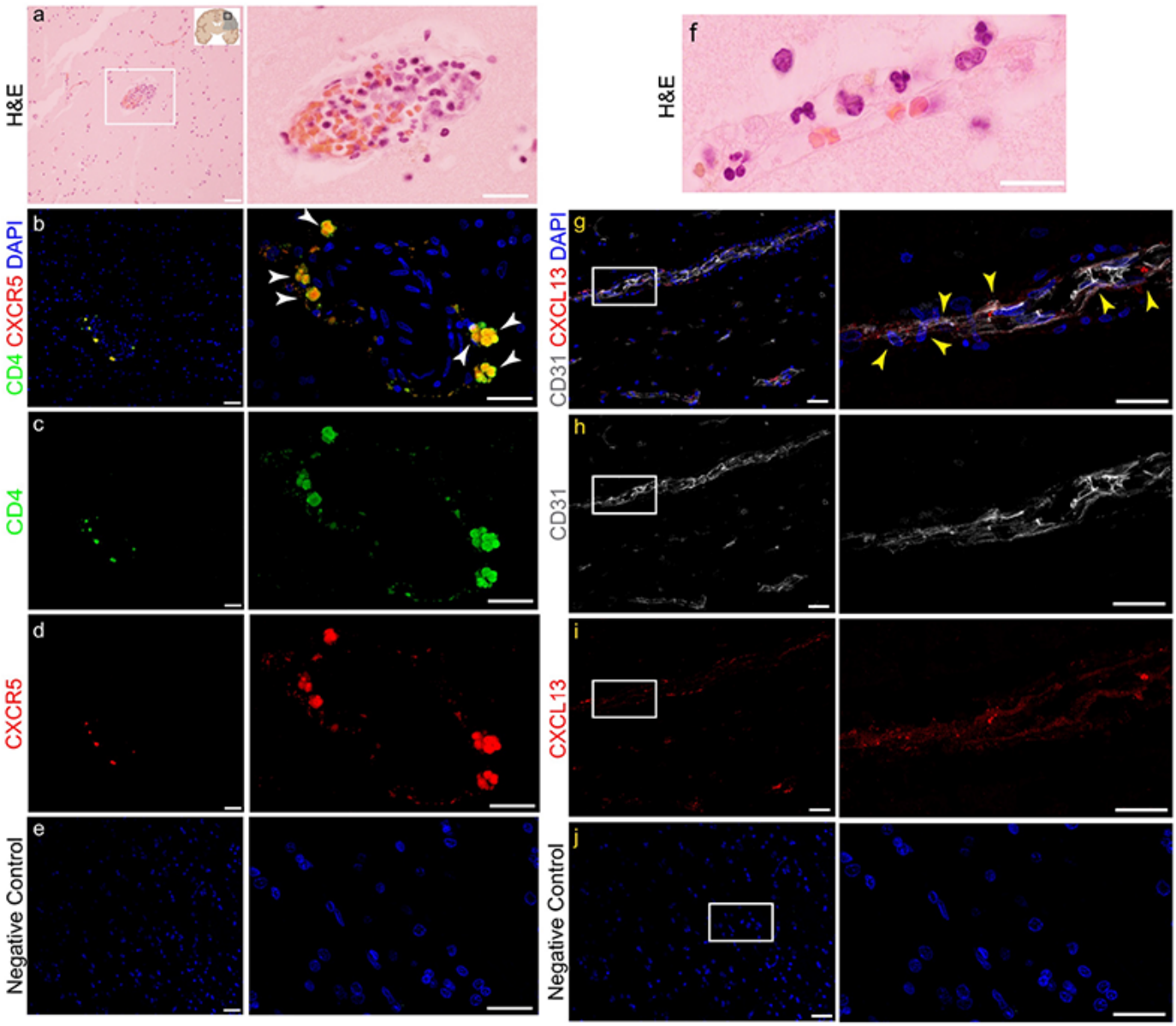

Figure 4

CXCR5+ CD4+ T cells and CXCL13+ vessels expressed in brain -peri-infarcts of human acute stroke patients. (a) Human acute stroke tissue stained with hematoxylin and eosin (H&E) depicting immune cell cluster within the brain. (b) Representative section stained with CD4 (green), CXCR5 (red), and DAPI (blue)

including CD4 (c) and CXCR5 (d) alone. Human acute stroke tissue stained with secondary only and DAPI (e). (f) Human acute stroke tissue stained with H&E depicting immune cell containing vessel within the brain. (g) Representative section stained with CD31 (white), CXCL13 (red), and DAPI (blue) including CD31 (h) and CXCL13 (i) alone. Human acute stroke tissue stained with appropriate secondary only and DAPI (e, j). Scale bar = 50 μm.

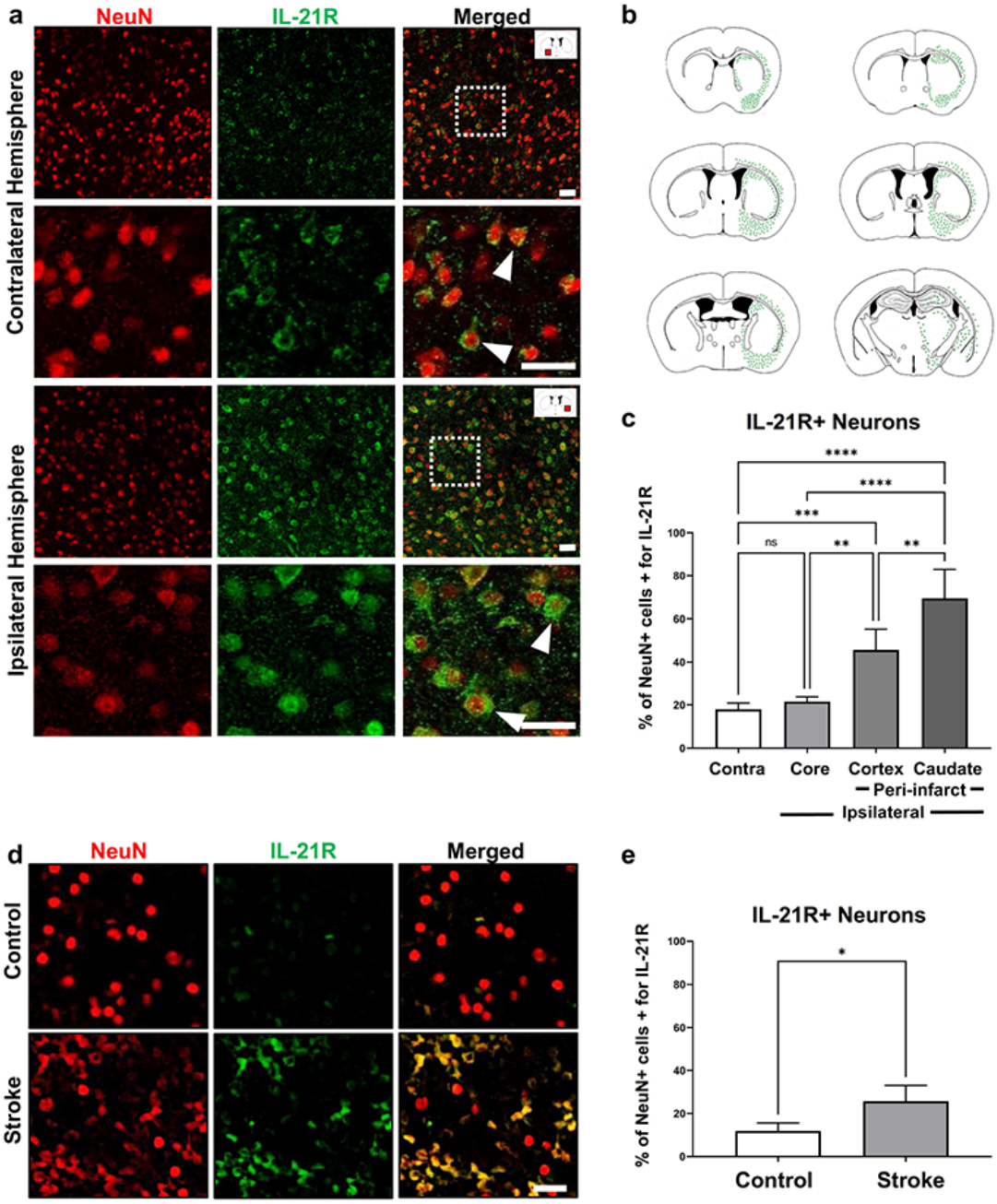

Figure 5

IL-21R is upregulated in the ipsilateral brain hemisphere of mice 24 hours after tMCAO in vivo and human stroke brains. (a) Low and high magnification representative images stained with NeuN (red), IL-21R (green), and Merged of contralateral brain hemisphere (top panels) and ipsilateral brain hemisphere (bottom panels) from mice 4hr after tMCAO. (b) Maps of IL-21R/NeuN double positive cells across coronal planes. Higher density of green dots represents higher number of double positive cells (n=6). (c) Quantification of the percentage of NeuN positive cells that were also positive for IL-21R in the contralateral hemisphere, ipsilateral core, ipsilateral peri-infarct (cortex) and the ipsilateral peri-infarct (caudate) (n=6). (d) High magnification representative images stained with NeuN (red), IL-21R (green), and Merged in human stroke brains (top) and control brains (bottom). (e) Quantification of the percentage of NeuN positive cells that were also positive for IL-21R in human stroke and control stroke brain. (n=4) Scale bar = 15 μm. Data represent mean ± s.e.m. *P < 0.05, **P < 0.01, ***P < 0.001, ****P < 0.0001. n.s. = not significant. One-way ANOVA followed by Dunn's post-hoc test (c) and Student's t test with Mann-Whitney U test (e).

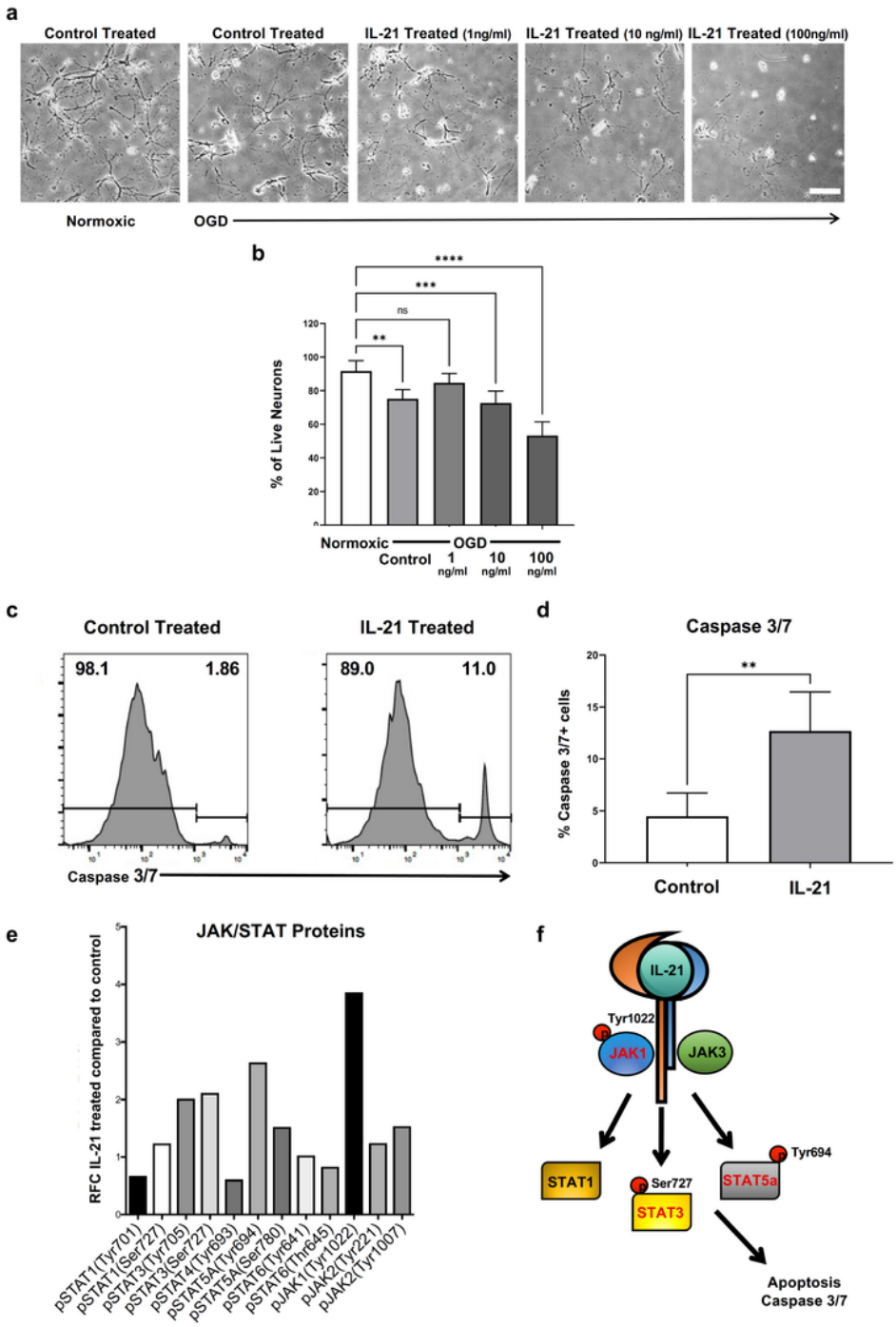

Figure 6

Administration of mIL-21 directly potentiates neuronal death following OGD conditions, induces Caspase 3/7 mediated apoptosis and activates JAK/STAT pathway in vitro. (a) Representative images of primary neurons under normoxic conditions (first panel), oxygen glucose deprivation (OGD) conditions followed by exposure to complete media alone for 24hrs (second panel), with mIL-21 at 1ng/ml (third panel), 10 ng/ml (fourth panel), and 100 ng/ml (last panel) Scale bar = 10 μm. (b) Quantification of primary neuron

survival following Normoxic conditions, OGD conditions followed by exposure to complete media for 24hrs, as well as OGD conditions followed to exposure to complete media with mIL-21 (1ng/ml, 10 ng/ml, and 100ng/ml) for 24hrs (n=5). (c) Representative flow cytometry histograms of Caspase 3/7 activity on primary neurons treated with OGD conditions for 90 min followed by 24hrs of normoxic conditions with control or mIL-21 (100ng/ml) for 24hrs. (d) Quantifications of the percentage of neurons expressing Caspase 3/7 activity. (n=5). (e) Relative fold change of JAK/STAT pathway related phosphorylated proteins following IL-21 treatment compared to control treated neurons in vitro. (f) Schematic of IL-21 activity on neurons. Data represent mean ± s.e.m. Data represent mean ± s.e.m. *P < 0.05, **P < 0.01, ***P < 0.001, ****P < 0.0001. n.s. = not significant. One-way ANOVA followed by Dunn's post-hoc test (b). Student's t test followed by Mann-Whitney U test (d).